PROCEEDINGS OF SCIENCE

Cosmology from EoR/Cosmic Dawn

Jonathan Pritchard[*1], **Kiyotomo Ichiki**[2], **Andrei Mesinger**[3], **Robert Benton Metcalf**[4], **Alkistis Pourtsidou**[4], **Mario Santos**[5], **Filipe Abdalla**[6], **Tzu-Ching Chang**[7], **T. Roy Choudhury**[8], **Xuelei Chen**[9], **Jochen Weller**[10], **Saleem Zaroubi**[11], **on behalf of the Cosmology-SWG and EoR/CD-SWG**

[1]*Imperial College London,* [2]*Nagoya University,* [3]*Scuola Normale Superiore, Pisa,* [4]*Universitá di Bologna,* [5]*University of the Western Cape,* [6]*University College London,* [7]*ASIAA,* [8]*NCRA,* [9]*National Astronomical Observatory of China,* [10] *Universitaets-Sternwarte Muenchen,* [11]*University of Groningen.*

E-mail: j.pritchard@imperial.ac.uk

SKA Phase 1 will build upon early detections of the EoR by precursor instruments, such as MWA, PAPER, LOFAR, and HERA, to make the first high signal-to-noise measurements of fluctuations in the 21 cm brightness temperature from both reionization and the cosmic dawn. This will allow both imaging and statistical maps of the 21cm signal at redshifts $z = 6-30$ and constrain the underlying cosmology and evolution of the density field. This era includes nearly 60% of the (in principle) observable volume of the Universe and many more linear modes than the CMB, presenting an opportunity for SKA to usher in a new level of precision cosmology. This optimistic picture is complicated by the need to understand and remove the effect of astrophysics, so that systematics rather than statistics will limit constraints.

This chapter will describe the cosmological, as opposed to astrophysical, information available to SKA Phase 1. Key areas for discussion include: cosmological parameters constraints using 21cm fluctuations as a tracer of the density field; lensing of the 21cm signal, constraints on heating via exotic physics such as decaying or annihilating dark matter; impact of fundamental physics such as non-Gaussianity or warm dark matter on the source population; and constraints on the bulk flows arising from the decoupling of baryons and photons at $z = 1000$. The chapter will explore the path to separating cosmology from 'gastrophysics', for example via velocity space distortions and separation in redshift. We will discuss new opportunities for extracting cosmology made possible by the sensitivity of SKA-1 and explore the advances achievable with SKA-2.

Advancing Astrophysics with the Square Kilometre Array
June 8-13, 2014
Giardini Naxos, Italy

*Speaker.

1. Introduction

The years since the COBE observations of the CMB have ushered in an age of precision cosmology. Key cosmological parameters have been determined by measurements of the distribution of matter in the Universe through WMAP and Planck observations of CMB anisotropies and large volume galaxy surveys such as SDSS. These surveys have made precision measurements of parameters describing the matter content of the Universe - the baryons Ω_b, dark matter Ω_c, dark energy Ω_Λ, radiation Ω_r, and neutrinos Ω_ν - and the physics of inflation - via the tilt n_s, amplitude A_s, running $\mathrm{d}n_s/\mathrm{d}\log k$ or the primordial potential power spectrum and r the ratio of tensor-to-scalar modes produced by inflation. These measurements have firmly established the basic picture of our Universe, known widely as the ΛCDM model of cosmology.

Despite this progress, measuring these numbers is only the first step towards a deep understanding of the underlying physics. Our ignorance of the nature of the dark matter and the dark energy or how neutrinos acquire mass and what value that mass takes are just two questions that modern cosmology hopes to address. Over the next decade two paths will help shed light on this. The simplest is simply to measure these cosmological parameters ever more precisely and over a wider range of times and scales in the hope of gaining further insights. The exemplar of this is with dark energy, where attempts to measure the redshift evolution of the dark energy density, parameterised by an equation of state $w(z)$, might distinguish a true cosmological constant from more general dark energy or modified gravity. For others there are critical thresholds of precision required to distinguish physical scenarios - for example, measuring the sum of the neutrino masses $M_\nu \lesssim 0.1$ would determine the neutrino mass hierarchy. Clearly more precision is a good thing, but it is not the only path forward.

Secondly, we can seek signatures of new physics in ways distinct from the distribution of large scale matter. The processes that produce dark matter will also allow it to annihilate and maybe to decay. The release of energy might have impact on the surrounding environment, heating the intergalactic medium. Pursuing unique signatures of new physics in new regimes will be a key part of the next decade.

The SKA is uniquely placed to probe cosmology as it is capable of mapping the Universe over wide volumes and an unprecedented range of redshifts. Figure 1 illustrates the additional range of volume and redshifts that the SKA will constrain. In this chapter, we will focus on the new opportunities created by SKA observations of the epoch of reionization (EoR) and the cosmic dawn (CD). This period has never before been observed offering a unique opportunity to test the consistency of the ΛCDM model and search for new hints to the great unanswered questions of cosmology.

Fundamental physics in cosmology is generally associated with the density field, whose fluctuations are generated by inflation and which contains imprint of other physics such as neutrino mass. Astrophysics is a major challenge to getting at cosmology with SKA, but we can identify several key approaches to extracting cosmology: (1) directly from density fluctuations (2) via the presence of exotic sources of radiation (3) via the radiation fields produced by all sources since those sources will trace the density field in some biased fashion (4) via the weak lensing of the 21cm signal by structures between the observer and signal (5) miscellaneous other probes. Extracting cosmology from the 21cm signal during the EoR will require a certain amount of cleverness to separate astro-

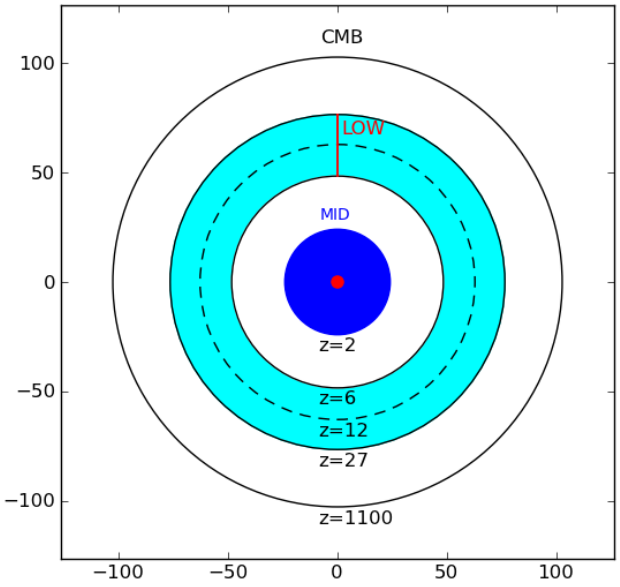

Figure 1: Illustration of the volume probed by SKA. 3D comoving volume mapped to a 2D circle. The volume probed by an all sky galaxy survey out to $z = 0.3$ (red circle, ∼SDSS) and $z = 2$ (blue circle, ∼SKA-MID) are marked as is the volume at the redshifts probed by SKA-LOW, $z = 6 - 27$ (cyan annulus).

physics from cosmology. Nonetheless the sensitivity of the instruments, large volume probed, and new redshift regime accessible to SKA makes this a very interesting area for new science.

In this chapter, we will explore these different avenues for extracting cosmology from the 21cm signal and attempt to assess the sort of constraints that will be achievable by SKA Phase 1 and 2. However, we caution the reader that this is not a settled area and it is still unclear how well astrophysics can be dealt with. New ideas may improve the constraints, but new obstacles may render them optimistic.

2. Cosmological parameters from density fluctuations

In this section, we explore the ability of SKA to constrain cosmological parameters via observations of the density field. Just as galaxy surveys constrain cosmology by using galaxies as a tracer of the linear density field, SKA can constrain cosmology by using the 21 cm brightness temperature as a tracer of the density field. This is not an unproblematic assertion, since brightness temperature fluctuations may be sourced by variation in the spin temperature and neutral fraction in addition to the density field.

$$\delta T_B = 27 x_{HI}(1+\delta_b)\left(\frac{T_S - T_{\rm CMB}}{T_S}\right)\left(\frac{1+z}{10}\right)^{1/2}\left[\frac{\partial_r v_r}{(1+z)H(z)}\right]^{-1} \text{mK} \qquad (2.1)$$

Equation 2.1 shows how these different terms come into play. In a regime where $T_S \gg T_{\rm CMB}$ and $x_H = 1$ then δT_B will be an unbiased tracer of the density field. At all other times the effects of astrophysics must be modelled and removed or somehow avoided. We will return to a discussion of this point in §7 as this is a critical point.

In this section, we take the optimistic view that there will a regime in which $\delta T_b \propto (1+\delta)$ so that the 21cm signal provides a clean measurement of the density field. This approach enables us to evaluate the best case scenario for SKA in measuring cosmological parameters. By comparing this to galaxy surveys we get a sense of how competitive SKA could be, if astrophysics could be overcome.

The sensitivity of a radio interferometer to the 21cm power spectrum has been well studied (e.g. Bowman et al. 2006; McQuinn et al. 2006; Mao et al. 2008) and we follow the same approach here. The variance of a 21 cm power spectrum estimate for a single **k**-mode with line of sight component $k_{||} = \mu k$ is given by (Lidz et al. 2008):

$$\sigma_P^2(k,\mu) = \frac{1}{N_{\rm field}}\left[\bar{T}_b^2 P_{21}(k,\mu) + T_{\rm sys}^2 \frac{1}{B t_{\rm int}} \frac{D^2 \Delta D}{n(k_\perp)} \left(\frac{\lambda^2}{A_e}\right)^2\right]^2. \tag{2.2}$$

The first term on the right-hand-side of the above expression provides the contribution from sample variance, while the second describes the thermal noise of the radio telescope. The thermal noise depends upon the system temperature $T_{\rm sys}$, the survey bandwidth B, the total observing time $t_{\rm int}$, the conformal distance $D(z)$ to the center of the survey at redshift z, the depth of the survey ΔD, the observed wavelength λ, and the effective collecting area of each antennae tile A_e. The effect of the configuration of the antennae is encoded in the number density of baselines $n_\perp(k)$ that observe a mode with transverse wavenumber $k_\perp$ (McQuinn et al. 2006). Observing a number of fields $N_{\rm field}$ further reduces the variance.

Estimates of the error on a power spectrum measurement are calculated using the Fisher matrix formalism, so that the $1-\sigma$ errors on the model parameter λ_i are $(\mathbf{F}_{ij}^{-1})^{1/2}$, where

$$F_{ij} = \sum_\mu \frac{\varepsilon k^3 V_{\rm survey}}{4\pi^2} \frac{1}{\sigma_P^2(k,\mu)} \frac{\partial P_{T_b}}{\partial \lambda_i} \frac{\partial P_{T_b}}{\partial \lambda_j}. \tag{2.3}$$

In this equation, $V_{\rm survey} = D^2 \Delta D(\lambda^2/A_e)$ denotes the effective survey volume of our radio telescopes and we assume wavenumber bins of width $\Delta k = \varepsilon k$. We will be interested in the cases where $\lambda_i = \{\bar{P}_{T_b}\}$ and $\lambda_i = \{P_{\mu^0}, P_{\mu^2}, P_{\mu^4}\}$.

We first illustrate the sensitivity of different iterations of SKA in Figure 2, where we take the parameters in Table 1 for SKA0 - with 50% of the SKA1 baseline collecting area, SKA1, and SKA2 - with x4 the collecting area of SKA1. For each of these we assume a filled core followed by r^{-2} distribution out to a maximum radius $R_{\rm max}$. HERA is assumed to have a uniform antennae distribution. SKA1 has 911 stations total with 899 in the core and 650 stations within a radius of 1km accounting for 75% of the total number of stations and collecting area. We limit to the innermost 850 within 2km, as the outer stations add little to the sensitivity. At lower frequencies the array is densely packed and has constant collecting area, at higher frequencies the array becomes sparse.

Table 1: Low-frequency radio telescopes and their parameters. We specify the number of antennae N_a, total collecting area $A_{\rm tot}$, bandwidth B, and total integration time $t_{\rm int}$ for each instrument. These values are fixed at $\nu = 110$MHz and extrapolated to other frequencies using $A_{\rm tot} = N_{\rm ant} N_{\rm dip} A_{\rm dip}$ with a physical station size of 35m and the number of antennae per station $N_{\rm dip} = 289$ and $A_{\rm dip} = \min(\lambda^2/3, 3.2\,{\rm m}^2)$.

Array	N_a	$A_{\rm tot}(10^3\,{\rm m}^2)$	B (MHz)	$t_{\rm int}$ (hr)	$R_{\rm min}(m)$	$R_{\rm max}(km)$
MWA	112	1.6	8	1000	4	0.75
LOFAR Core	48	38.6	8	1000	100	1.5
HERA	331	50.0	8	1000	14.3	0.3
SKA0	850×0.5	290×0.5	8	1000	35	2
SKA1	850	290	8	1000	35	2
SKA2	850×4	290×4	8	1000	35	2

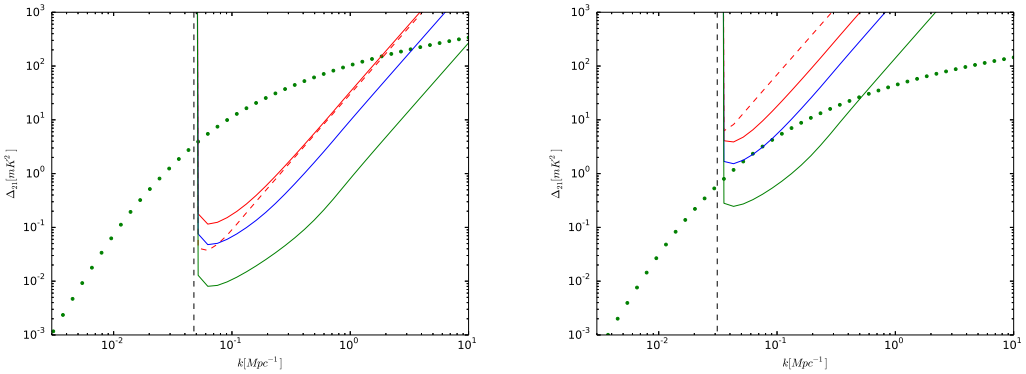

Figure 2: Sensitivity plots of HERA (red dashed curve), SKA0 (red), SKA1 (blue), and SKA2 (green). Dotted curve shows the predicted 21cm signal from the density field alone assuming $x_H = 1$ and $T_S \gg T_{\rm CMB}$. Vertical black dashed line indicates the smallest wavenumber probed in the frequency direction $k = 2\pi/y$, which may limit foreground removal. *Left panel:* $z = 8$ *Right panel:* $z = 20$.

Figure 2 illustrates a few key points governing parameter constraints. Here we have eliminated modes whose wavelength exceeds the instrument bandwidth removing sensitivity to the largest physical scales (smallest k modes). At $z = 8$, SKA0 is directly comparable in sensitivity to the proposed HERA experiment Pober et al. (2014), which is more centrally concentrated to compensate for its small number of stations. By $z = 20$ the amplitude of the 21 cm signal is too small to be detected by SKA1 *if we assume* $T_S \gg T_\gamma$. Detection of the 21cm signal at $z \gtrsim 20$ with SKA1 is dependent upon a strong 21cm absorption signal that boosts the amplitude of the 21cm power spectrum. Unfortunately, it seems likely that during the absorption regime the details and spatial variation of the spin temperature will matter and complicated getting at cosmology.

The key parameters for determining cosmological parameters are the effective volume probed and the minimum wavenumber probed $k_{\rm min}$ where modes can still be assumed to be linear. SKA has a significant advantage over galaxy surveys as more modes are still in the linear regime at $z > 6$.

We set $k_{\rm min} = 2{\rm Mpc}^{-1}$ at $z = 8$ corresponding to the scale where $\sigma(2\pi/k) = 0.5$.

Table 2 shows the cosmological parameters obtained with the listed experimental performances. The key take home message of this is that SKA-LOW has the raw sensitivity to add useful information on cosmological parameters to Planck. The largest gains are on parameters that require small scale information - the running of the primordial power spectrum and neutrino masses, for example. This also indicates that SKA-LOW will have the sensitivity to provide a useful consistency check on cosmological parameters from the high redshift regime long before dark energy becomes important.

Table 2: Fiducial parameter values and $1-\sigma$ experimental uncertainties for cosmological parameters. Dashes indicate parameters not relevant for that experiment; ∞ indicates parameters that are relevant, but not constrained.

Parameter	$\log\Omega_m h^2$	$\log\Omega_b h^2$	Ω_Λ	n_s	$\log A_s$	$dn_s/d\log k$	τ
Value	-1.92	-3.79	0.7	0.95	-0.186	0	0.1
planck	0.00767	0.0059	0.00899	0.00303	0.00888	0.00467	0.00426
hera	0.00732	0.00568	0.00644	0.00291	0.00867	0.00408	0.00422
ska1 50	0.00732	0.00532	0.00829	0.00298	0.00836	0.0028	0.00412
ska1	0.00198	0.00425	0.00237	0.00193	0.00799	0.000827	0.00399
ska 400	0.00103	0.00425	0.00189	0.00185	0.00797	0.00073	0.00398

We make no attempt here to model the effects of astrophysics on these constraints. Increasingly conservative assumptions can degrade these constraints arbitrarily far. Nonetheless it is clear that the attempt to extract cosmological information could be quite rewarding.

Beyond the standard cosmological parameters there are exotic physics that can only be probed at high redshift, since its effect decreases with time. Compensated isocurvature modes are a one example, where the contribution of the isocurvature does not grow with time and so becomes negligible compared to the growing adiabatic mode at late times (Gordon & Pritchard 2009).

3. Constraining new physics from heating

The 21cm signal probes both the ionization and thermal state of the IGM. Although we do not know the precise timing and evolution of the signal, empirical scaling relations based on local star-forming galaxies (e.g. Mineo et al. 2012) suggest that the X-rays from early galaxies heat the IGM to temperatures above the CMB before the bulk of reionization (e.g. Furlanetto 2006; McQuinn & O'Leary 2012). This marks the transition of the 21cm signal from absorption to emission, with large-scale fluctuations in gas temperature likely driving the 21cm power to its largest amplitude (e.g. Pritchard & Furlanetto 2007; Baek et al. 2010). The epoch of IGM heating is a powerful probe of the high-energy processes in the early Universe, with could have both astrophysical and cosmological origins. Both can tells us about the nature of dark matter (DM).

In order to explain the apparent deficiencies of CDM on small (sub-Mpc) scales, Warm Dark Matter (WDM) models have recently gained in popularity. In these models, DM is assumed to consist of smaller mass particles, $\sim$ keV, such as the sterile neutrino or gravitino. The increased

particle free-streaming and velocity dispersion (acting as a sort of effective pressure), can dramatically suppress structures on small-scales. This suppression is even more obvious in the early Universe, where typical halos hosting galaxies were much smaller, and larger structures did not have time to fragment. Current astrophysical lower limits on the WDM particle range from $m_x \gtrsim$ 1-3 keV (assuming a thermal relic relativistic at decoupling), with various degrees of astrophysical degeneracy (e.g. de Souza et al. 2013; Kang et al. 2013; Pacucci et al. 2014; Viel et al. 2013)

The resulting dearth of galaxies in the early Universe means that the astrophysical epochs in the 21cm signal were delayed. The challenge as always will be to disentangle the cosmological impact from astrophysical uncertainties, such an a lower than expected star formation efficiency in CDM. Since the fractional suppression of structure increases with redshift, this becomes much easier with the first galaxies observable with the SKA. For example, we only need to understand the astrophysics of the first galaxies to an order of magnitude in order to improve on current m_X constraints (Sitwell et al. 2014) Moreover, even if the star-formation efficiency in CDM is allowed to vary in order to mimic the mean 21cm evolution in WDM models, the signal will still not be completely degenerate (see Fig. 3a). This is due to the fact that the galaxies driving the 21cm evolution in WDM should reside in higher mass, more rapidly evolving halos, than those in CDM. The increased bias of such halos results in a larger 21cm fluctuations (see Fig. 3a).

The heating of the IGM could also have a cosmological component. In particular, annihilations of dark matter particles in the $\sim$ 10 GeV mass range (motivated by recent results from indirect experiments; (e.g. Adriani et al. 2009; Abdo et al. 2010; Aguilar et al. 2013) could provide a dominant source of heat, before the birth of the first galaxies. Driven by the evolution of $\sim M_\cdot$ structures, several orders of magnitude smaller than those hosting galaxies, heating is expected to be much slower in such models, resulting in a smaller brightness temperature gradient $\mathrm{d}\delta T_b/\mathrm{d}\nu \sim 4\mathrm{mK\,MHz}^{-1}$ in the range $\nu \sim 60-80$ MHz (Valdés et al. 2013). Moreover, DM annihilations would heat the IGM quite uniformly, which is not the case for heating driven by astrophysical sources residing in early galaxies. The resulting lack of temperature fluctuations (see Fig. 3b) would result in dramatic drop in 21cm power during heating, which would be easy to identify with the SKA (Evoli et al. 2014). Furthermore, the ensuing rise in 21cm power when the galaxies start contributing to heating the IGM should occur *when the IGM is already in emission*. The later is a qualitatively robust signature of DM annihilation heating, easily obtainable with the SKA.

3.1 21 cm signal from the PMFs

Primordial magnetic fields (PMFs) has been intensively investigated in the literature as possible seeds for large scale magnetic fields observed in galaxies and clusters of galaxies (for a recent review, see Durrer & Neronov (2013)). Magnetic fields in galaxies in high redshifts Bernet et al. (2008) and in void regions Neronov & Vovk (2010); Ando & Kusenko (2010); Takahashi et al. (2013) can well be the pieces of evidence that the seed fields are of primordial origin. The primordial magnetic fields may be created in the very early universe, e.g., at the epoch of inflation, cosmological phase transition, and cosmological recombination. The Planck collaboration recently places limits on the PMFs as $B_{\lambda=1\mathrm{Mpc}} < 3.4$ nG and $n_B < 0$ from the temperature anisotropies on large and small angular scales Planck Collaboration (2013).

The CMB brightness temperature fluctuations produced by the neutral hydrogen 21-cm line (21 cm) would offer a new probe of the primordial magnetic fields (PMFs) created in the early

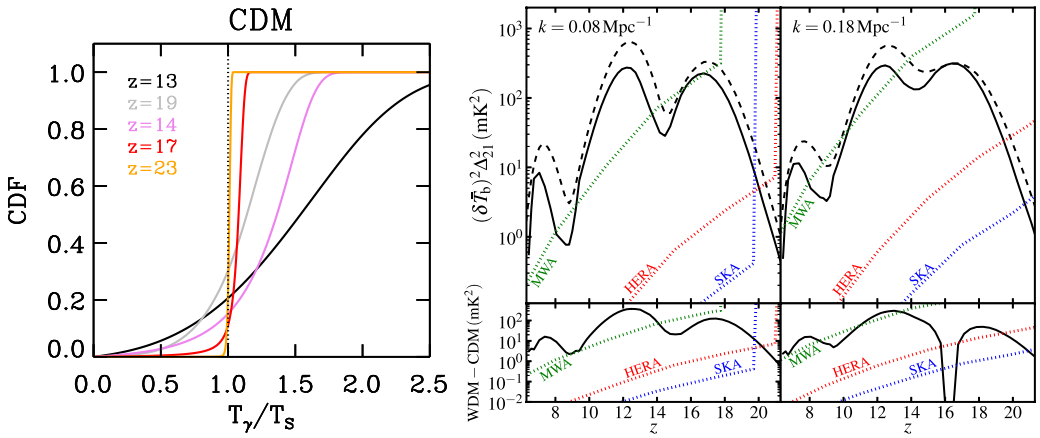

Figure 3: *Right panel:* Evolution of the power spectrum of δT_b for WDM with $m_X = 2$ keV. The top panels show power spectra at $k = 0.08, 0.18$ Mpc^{-1} for WDM (dashed) and the CDM model (solid). CDM models have f_*(z) (star-formation efficiency) chosen to reproduce the global 21-cm signal found for the respective WDM model. The bottom panels show the difference in the power spectrum between WDM and CDM models. Dotted curves show forecasts for the 21cm power spectrum thermal noise as computed in Mesinger et al. (2014) assuming 2000 h of observation time. The dotted green, blue and red curves are the forecasts for the MWA, SKA and HERA, respectively. This figure is from Sitwell et al. (2014). CDFs of T_γ/T_S corresponding to the fiducial and extreme astrophysical X-ray heating (black and gray curves respectively) from Mesinger et al. (2013). The colored curves correspond to models in which 10 GeV DM annihilations are also accounted for (in addition to fiducial astrophysical heating), with varying relative contribution. The curves correspond to the redshift for which $T_s \sim T_{\rm CMB}$. Figure is from (Evoli et al. 2014).

universe. For the 21 cm observation, aside from the early structure formation effect by the Lorentz force from the PMFs, one of the important effects is the dissipation process of the PMFs that increases the baryon temperature. The dissipation occurs mainly through the ambipolar diffusion due to the velocity difference between neutral hydrogen (which is the dominant component in the dark ages) and ionized particles (whose trajectory is bent by the Lorentz force). The effect of the dissipation is rather significant. The gas temperature can reach 1000 K or even 10^4 K at $z = 30$ if the magnetic fields have the strength of $B_\lambda \sim 3$ nG Sethi & Subramanian (2005); Tashiro & Sugiyama (2006); Schleicher et al. (2009); Kunze & Komatsu (2014).

This dissipation will give rise to a unique signature of the PMFs on the 21 cm observation. Because the spin temperature is closely coupled to the gas temperature at high redshift ($z > 30$), the 21 cm signal would come as 'emission' if the energy dissipation is efficient. In Fig. 4 the global HI signal with several magnetic field strengths are shown. For cases with sufficient magnetic fields, say $B \gtrsim 0.03$ nG, the signal is always emission against CMB while in the standard ΛCDM model the signal would be absorption for the frequency range of $f_\nu \lesssim 80$ MHz (corresponding to the signal from redshift $z \gtrsim 20$).

We show the angular power spectrum of the 21 cm brightness temperature including the PMFs in Fig. 4b Shiraishi et al. (2014). Here we do not account for any (standard) heating effects (i.e., UV, X, and Lα background emissions) to isolate and clarify the effects from the PMFs. On large scales which may be relevant to SKA observations, there are two distinct contributions. One is from the

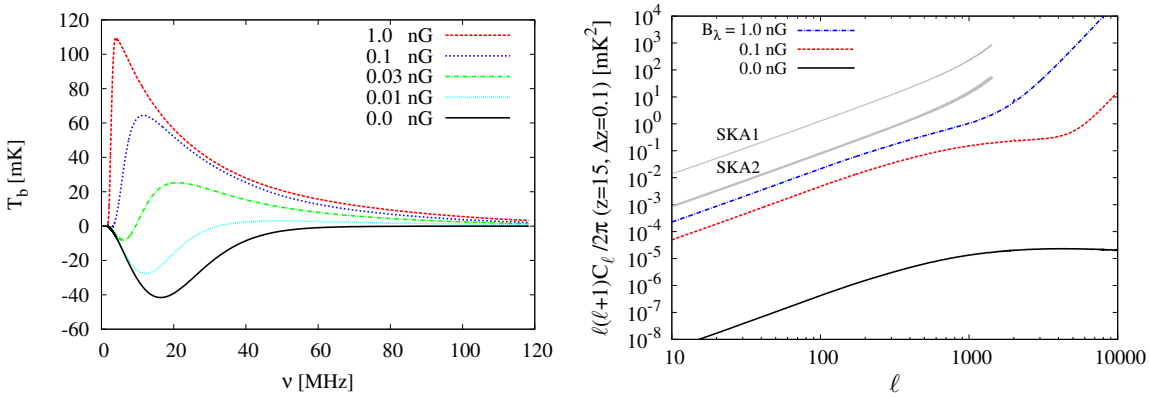

Figure 4: *Left panel:* The global 21 cm signal with magnetic field strength $B = 1$ 0.1, 0.03, and 0.01 nG (colored lines from top to bottom). The solid line corresponds to the model without primordial magnetic fields. Note that any other heating source than magnetic fields is neglected in the figure. *Right panel:* Angular power spectra for PMF strengths: $B = 0,\ 0.1,\ 1.0$ nG at $z = 15$. The bottom curve shows the power spectrum from the standard density perturbations for fully neutral medium without any heating and reionization processes. The red and blue curves correspond to the cases with heating by the PMFs with $B = 0.1$ nG and $B = 1.0$ nG, respectively. The heating induces deviations of the spin temperature from the CMB temperature and the signal is enhanced. The noise curves for SKA1 and SKA2 are also shown as indicated. By courtesy of M. Shiraishi & H. Tashiro.

standard (adiabatic) density fluctuations enhanced by the heating from the PMFs, and the other is from the PMF induced density fluctuations dominant on smaller scales Tashiro & Sugiyama (2006); Schleicher et al. (2009). We can see from the figure that $B = 1$ nG magnetic fields are marginally within reach for a statistical detection of the power spectrum. Stacking observing channels in principle will add more statistical power.

The angular correlation function in real space including the effects from the PMFs is also studied in Sethi & Subramanian (2009). The function exhibits a distinct feature because the PMFs induce early structure formation and the small scale halos form more compared to the case in the standard ΛCDM model The signal from primordial magnetic fields shows oscillatory feature contrary to that in the standard ΛCDM since the matter power spectrum induced by the PMFs is blue and most of halos are formed at the scale close to the magnetic Jeans' length. It has been argued that 5 sigma detection of the 0.5 nG magnetic fields will be possible with less than one week integration of SKA observation Sethi & Subramanian (2009).

4. Bulk flows

Tseliakhovich & Hirata (2010) demonstrated the existence of coherent supersonic velocity flows between baryons and dark matter after decoupling at $z \approx 1100$. This has the consequence of inhibiting the formation of star forming galaxies in low-mass halos ($M \lesssim 10^6\,\mathrm{M}_\odot$) (e.g. Maio et al. 2011; Stacy et al. 2011). If there is significant star formation in such halos, dependent upon H_2 cooling and the absence of Lyman-Werner background, then the radiation from such galaxies can lead to a significantly enhanced 21cm signal (Visbal et al. 2012; Fialkov et al. 2014; McQuinn & O'Leary 2012). While the details of this are still quite uncertain, if this enhancement exists

it opens the possibility of measuring cosmology at $z = 20 - 27$ with SKA. The relative velocity flows trace the sound horizon and so especially enhance the baryon acoustic oscillation feature in the 21cm power spectrum (see e.g. McQuinn & O'Leary 2012). The BAO signature provides a standard ruler, calibratable with CMB observations, to form an inverse distance ladder stretching from $z = 1100$ through $z \sim 20$. Such measurements would strongly constrain the parameter space for departures from ΛCDM, such as early dark energy models (e.g. Bartelmann et al. 2006; Doran & Robbers 2006). Imaging the 21cm structures induced by these bulk flows will be possible with both SKA-LOW Phase 1 and the full SKA. This will be a truly novel probe of cosmology at high redshift vastly the reducing the possibility that non-standard dynamics could hide in the observational void between low redshift galaxy surveys and the CMB.

5. Cosmology on ultra-large scales with SKA-Low

The measurement of very large scales provides an unique way to probe modifications to the standard cosmological model. In particular it is on scales past the matter-radiation equality peak that General Relativistic corrections become important, at scales above ~ 5 comoving Gpc/h (Jeong et al. 2012). Probing this region would allow to check for any inconsistencies in General Relativity. However, current surveys are still far from probing this region - as an example, the BOSS survey only probes scales up to 200 Mpc/h (Anderson et al. 2012). Moreover, primordial non-Gaussianity will affect the clustering of biased tracers of dark matter, by adding an extra correction $\Delta b_X(z,k)$ to the Gaussian large-scale bias b_X^G of a given biased tracer X: $\Delta b_X(z,k) = 3[b_X^G(z) - 1]\Omega_m H_0^2 \delta_c / [c^2 k^2 T(k) D_+(z)] f_{nl}$. Here, $\Omega_m = \Omega_b + \Omega_{dm}$ is the total (baryons plus dark matter) matter fraction, H_0 is the Hubble constant, $\delta_c \simeq 1.686$ is the critical collapse density contrast of matter, $T(k)$ is the matter transfer function versus the physical wave number k, and $D_+(z)$ is the linear growth factor of density perturbations. Attempts at detecting this effect with redshift surveys have led to some constraints on f_{nl} (Giannantonio et al. 2014).

By observing at very high redshifts, a low frequency interferometer would be able to probe these large 3-dimensional scales during the Epoch of Reionization and beyond. Although astrophysics will generate model dependent features on the 21cm power spectrum, it is expected that on large enough scales the power spectrum should follow the dark matter one with a different amplitude. For instance, during the epoch of reionization, the ionisation power spectrum should be a biased linear tracer of the dark matter one on scales much larger than the bubble size (see Figure 5. Although the bias itself will depend on the assumed astrophysical model, measurements on these scales will allow to pick any scale dependence generated by primordial non-Gaussianity or General Relativistic corrections.

By accessing these large volumes, probes of the high-z 21cm signal will not only measure these large scales but also have enough modes to reduce cosmic variance on the scales of interest. Having large fields of view will therefore be a key factor for these experiments. The field of view of SKA1-Low ranges from 7 deg^2 at 220 MHz ($z \sim 5.5$) to 133 deg^2 at 50 MHz ($z \sim 27$), going basically as $(1+z)^2$. These correspond to scales of ~ 380 comoving Mpc at $z \sim 5.5$ to ~ 2.3 comoving Gpc at $z \sim 5.5$. As a further example, a fixed redshift bin of 0.1 would evolve on the same range from 50 Mpc to 5.5 Mpc (decreasing with z). We see therefore that, although the volumes accessible by SKA1-Low are quite large, especially at very high-z, we would require a

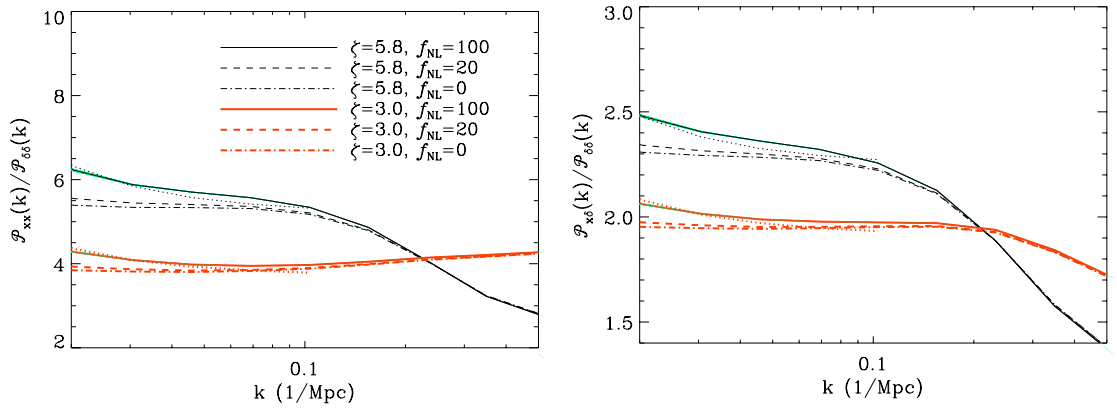

Figure 5: Ionization power spectra with non-Gaussianity of the local form from numerical simulations. We show $f_{nl} = (0, 20, 100)$ (dot-dashed, dashed, solid) for efficiency $\zeta = (5.8, 3.0)$ (thin black, thick red) at $z = 7.5$, where $x_{\rm HI} = (0.50, 0.75)$. Analytical fits are in dotted lines.

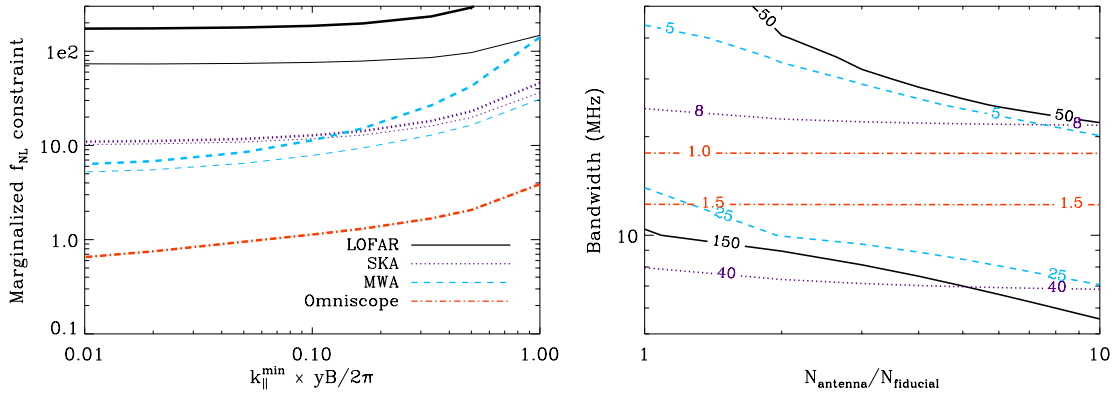

Figure 6: *Top*: Marginalized f_{nl} constraints for cases with noise (thick) and without noise (thin), which overlap for Omniscope. We consider a bandwidth of 6 MHz, but assume foregrounds can be removed on scales larger than $k_\parallel = 2\pi/(yB)$. *Bottom*: Marginalized f_{nl} constraints as function of bandwidth and number of antennae. The bandwidth limits the number of modes and largest scale probed along the LOS (via the survey volume $V \propto B$ and $k_\parallel^{\rm min} \propto 1/B$), whereas a larger number of antennae for fixed array density increases the survey resolution and number of perpendicular modes (via $n(u_\perp)$, on large scales $\propto N_{\rm ant}$, and $u_\perp^{\rm max} \propto \sqrt{N_{\rm ant}}$). The color coding is the same as for the top panel.

telescope with about 100 deg^2 at $z \sim 8$ to probe Gpc scales. Something that will probably have to wait for SKA2. Figure 6 shows the constraints on the primordial non-Gaussianity parameter for different telescopes.

6. Cosmic shear and the EoR

It is possible that the EoR signal could be used to measure weak gravitational lensing. In Zahn & Zaldarriaga (2006) and Metcalf & White (2009) it was shown that if the EoR is at redshift $z \sim 8$ or later, a large radio telescope such as the SKA could measure the lensing convergence power spectrum. However a very large $f_{\rm sky}$ and a very compact low frequency array was assumed by those

authors. Here the calculation is repeated with parameters that are more consistent with current SKA plans. The current plans for a 25 square degree survey with SKA1-Low will preclude making competitive measurements of the cosmological parameters through their effects on the weak lensing power-spectrum because of sample variance (this is not true of the SKA1-Mid at lower redshift where the survey area will be much larger.) It still might be possible to map the lensing convergence within the 25 square degree EoR survey area. This would allow us to actually "see" the distribution of dark matter in a typical region of the sky, something that is only possible with galaxy lensing around very atypical, large galaxy clusters. This would provide a great opportunity to correlate visible objects with mass and test the dark matter paradigm.

The previously mentioned authors extended the Fourier-space quadratic estimator technique, which was first developed in Hu (2001) for CMB lensing observations to three dimensional observables, i.e. the 21 cm intensity field $I(\theta,z)$. The convergence estimator and the corresponding lensing reconstruction noise are calculated assuming that the temperature (brightness) distribution is Gaussian. This will not be strictly true during the EoR, but serves as a reasonable approximation for these purposes. Note that the lensing reconstruction noise contains the thermal noise of the telescope which -assuming a uniform telescope distribution- is calculated using the formula

$$C_\ell^{\rm N} = \frac{(2\pi)^3 T_{\rm sys}^2}{B t_{\rm obs} f_{\rm cover}^2 \ell_{\rm max}(\nu)^2}\,, \tag{6.1}$$

where the system temperature $T_{\rm sys}$ at high redshifts is dominated by galactic synchrotron radiation and can be approximated by $T_{\rm sys} = 60\times(\nu/300\,{\rm MHz})^{-2.55}\,{\rm K}$ Dewdney (2013), B is the chosen frequency window, $t_{\rm obs}$ the total observation time, $D_{\rm tel}$ the diameter (maximum baseline) of the core array, $\ell_{\rm max}(\lambda) = 2\pi D_{\rm tel}/\lambda$ is the highest multipole that can be measured by the array at frequency ν (wavelength λ), and $f_{\rm cover}$ is the total collecting area of the core array $A_{\rm coll}$ divided by $\pi(D_{\rm tel}/2)^2$.

The advantage of 21cm lensing is that one is able to combine information from multiple redshift slices. In Fourier space, the temperature fluctuations are divided into perpendicular to the line of sight wave vectors $\mathbf{k}_\perp = \mathbf{l}/r$, with r the angular diameter distance to the source redshift, and a discretized version of the parallel wave vector $k_\parallel = \frac{2\pi}{\mathscr{L}} j$, where $\mathscr{L}$ is the depth of the observed volume. Considering modes with different j independent, an optimal estimator can be found by combining the individual estimators for different j modes without mixing them. The three-dimensional lensing reconstruction noise is then found to be (Zahn & Zaldarriaga 2006)

$$N(L,\nu) = \left[\sum_{j=1}^{j_{\rm max}} \frac{1}{L^2}\int \frac{d^2\ell}{(2\pi)^2}\frac{[\mathbf{l}\cdot\mathbf{L}C_{\ell,j} + \mathbf{L}\cdot(\mathbf{L}-\mathbf{l})C_{|\ell-L|,j}]^2}{2C_{\ell,j}^{\rm tot}C_{|\mathbf{l}-\mathbf{L}|,j}^{\rm tot}}\right]^{-1}. \tag{6.2}$$

Here, $C_{\ell,j}^{\rm tot} = C_{\ell,j} + C_\ell^{\rm N}$, where $C_{\ell,j} = [\bar{T}(z)]^2 P_{\ell,j}$ with $\bar{T}(z)$ the mean observed brightness temperature at redshift z due to the average HI density and $P_{\ell,j}$ the underlying dark matter power spectrum (Zahn & Zaldarriaga 2006). For SKA1-Low we can consider a $1,000$ hr observation time and we choose $B = 8\,{\rm MHz}$ and $j_{\rm max}\sim 40$, but with multiple bands ν that can be stacked to reduce the noise so that $N_L = 1/\sum_\nu [N(L,\nu)]^{-1}$.

At redshift $z_s\sim 8$, we can assume the SKA1-Low Baseline Design (Dewdney 2013) parameters of $A_{\rm coll}\simeq 0.3\,{\rm km}^2$ with maximum baseline $D_{\rm tel} = 4\,{\rm km}$, while for SKA we can consider $A_{\rm coll}\simeq 1.2\,{\rm km}^2$. The estimated lensing noise is shown in Figure 7 along with the estimated signal. Here

$C_L^{\kappa\kappa}$ is the convergence field power spectrum at $z_s = 8$ and N_L the lensing reconstruction noise assuming a reionization fraction $f_{\rm HI} = 1$.

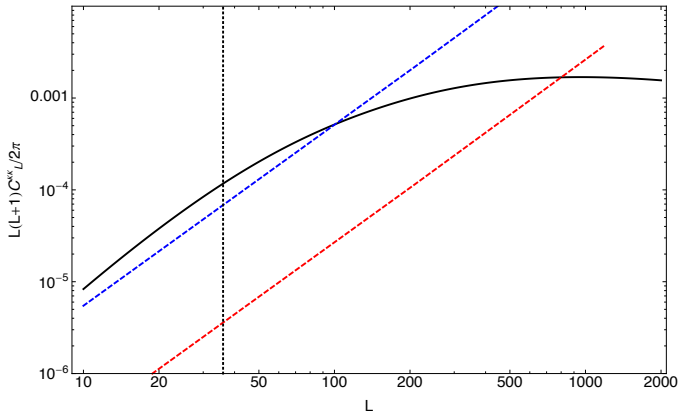

Figure 7: The lensing convergence field power spectrum, $C_L^{\kappa\kappa}$, for sources at $z = 8$ is shown as a solid black line and lensing reconstruction noise N_L as dashed lines. The blue dashed line is for SKA1-Low with 10 8 MHz frequency bins around $z = 8$ spanning the redshift range $z \simeq 6.5 - 11$. The red dashed line is for SKA and the same frequency bins. The vertical line is approximately the lowest L accessible with a 5-by-5 degree field. Where the noise curves are below $C_L^{\kappa\kappa}$, typical fluctuations in the lensing deflection should be recoverable in a map.

These results show that it might be possible to map the lensing signal over a range of angular scales. This measurement greatly benefits from the larger collecting area that will come with Phase 2 of the SKA (we also note that considering a more compact array, i.e. smaller $D_{\rm tel}$, also improves the signal-to-noise). The weak lensing power spectrum can be better measured for redshifts after reionization using SKA-Mid and the same 21 cm intensity mapping technique discussed, but over a much larger area of sky (Pourtsidou & Metcalf 2014).

7. Separating “gastrophysics" and cosmology

The key challenge for extracting fundamental physics from the 21cm signal will be separating the effects of cosmology from “gastrophysics". A number of avenues have been studied in the literature, which broadly separate into (1) avoidance and (2) modelling. In the absence of a clearly defined window where $T_S \gg T_{\rm CMB}$ and $x_H = 1$ it might still be possible to avoid astrophysics via the angular dependence of the power spectrum induced by redshift space distortions. Focussing on the $P_{\mu^4} \approx P_\delta$ part could lead to clean cosmological measurements. Obtaining precision cosmology this way is hard and the literature suggests little improvement over Planck is possible (McQuinn et al. 2006; Mao et al. 2008). Figure 8 shows predicted errors bars for SKA1 on the P_{μ^2} and P_{μ^4} parts of the power spectrum. A detection is possible with reasonable sensitivity at wavenumbers $k = 0.1 - 1\,{\rm Mpc}^{-1}$.

$$P(k) = P_{\mu^0}(k) + P_{\mu^2}\mu^2 + P_{\mu^4}\mu^4 \tag{7.1}$$

Information in P_{μ^2} is likely to help with modelling of the astrophysics. As will information from different redshift slices, which when combined may make it possible to characterise the astro-

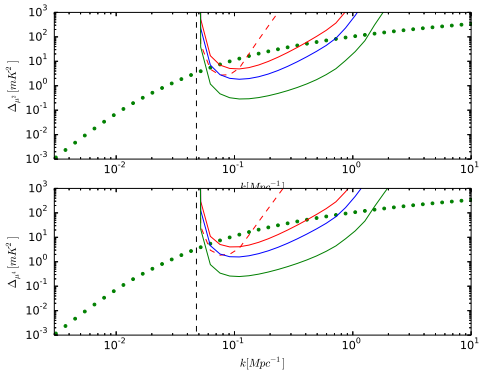

Figure 8: Sensitivity plots on P_{μ^2} and P_{μ^4} for HERA (red dashed curve), SKA0 (red), SKA1 (blue), and SKA2 (green). Dotted curve shows the predicted 21cm signal from the density field alone assuming $x_H = 1$ and $T_S \gg T_{\rm CMB}$. Vertical black dashed line indicates the smallest wavenumber probed in the frequency direction $k = 2\pi/y$, which may limit foreground removal. *Left panel:* $z = 8$ *Right panel:* $z = 20$.

physics on large scales. This has yet to be examined in detail and it is unclear how well modelling of astrophysics propagates into cosmological parameter uncertainties.

Compared with the CMB our theoretical understanding of the 21cm signal during reionization is poor. Predictions for the 21cm power spectrum do not exist at the same level of precision as the cosmology. Nonetheless, we expect the contribution of astrophysics to be relatively broad band and determined by extra power about a characteristic scale, eg the bubble size during reionization.

8. Paths to cosmology with Phase 1 and Phase 2

Short section to comment on what Phase 2 gets you over Phase 1.

9. Conclusions

SKA-LOW will provide the first window onto cosmological information from the epoch of reionization and cosmic dawn. This makes it unique among the diverse array of future cosmological experiments, which are limited to redshfits $z \lesssim 3$. This new view of the Universe will test the standard cosmological model deep in the matter dominated regime, where, in principle, we believe we know the evolution of the Universe. Deviations from ΛCDM predictions would signal new physics. Cosmology with SKA-LOW has potential to be very interesting, but will also be hard.

The large volume and number of linear modes of the density field accessible at high redshift will one day lead to revolution in precision cosmological constraints. SKA-LOW Phase 1 will take the first step in this direction, but will be limited by the relatively small sky areas it can survey; SKA2 will push significantly further. It remains to be seen how significantly astrophysics limits our ability to extract cosmology from the density field itself, but it is clear that the effort should be made. The real gain here is unlikely to be in refining how accurately we know ΛCDM parameters, but in testing the paradigm in a new regime.

Much clearer is the ability of both SKA-Low Phase 1 and 2 to measure the thermal history of the Universe at redshifts $z = 6 - 27$. As elucidated in Section 3 the thermal history contains information about exotic physics - dark matter physics, primordial magnetic fields, and more. The spatial variation of such heating, different from that of galaxies, provides a clear signature of novel physics. SKA will be able to identify and characterise such signatures constraining new physics.

Bulk flows..

Large volumes accesses super-horizon physics and with SKA it will be possible to search for relativistic corrections and primordial non-Gaussianity on $\gtrsim$ Gpc scales.

Since the 21cm signal must pass through the intervening density field, weak lensing will allow SKA to map out the dark matter field. The key advantage here is that the 21cm signal is a diffuse background so that representative parts of the Universe at high redshift can be mapped, rather than extreme regions in the vicinity of galaxy clusters.

In this chapter, we have focussed on the main paths to cosmology with SKA-LOW. There are other ideas extant or possible. For example, constraining time evolution of the fine structure constant (Khatri & Wandelt 2007) or observing cosmic strong wakes (Brandenberger et al. 2010). 21cm observations over wide sky areas offer a way of probing distinct Hubble volumes in the same way as the CMB. Given the relative infancy of this field, it is likely that new ideas for probing cosmology will be developed during the development of SKA.

It is hopefully clear that SKA-LOW will have something to say on a wide range of cosmological topics. The context is quite different from traditional probes of cosmology, so that the subtleties of cosmology from 21cm observations are not fully understood. It seems unlikely that SKA-LOW will transform our understanding of cosmology, but cosmology with SKA-LOW will be very interesting.

References

Abdo, A. A. et al. 2010, JCAP, 4, 14

Adriani, O. et al. 2009, Nat., 458, 607

Aguilar, M. et al. 2013, Physical Review Letters, 110, 141102

Anderson, L. et al. 2012, MNRAS, 427, 3435

Ando, S. & Kusenko, A. 2010, ApJ, 722, L39

Baek, S., Semelin, B., Di Matteo, P., Revaz, Y., & Combes, F. 2010, A & A, 523, A4

Bartelmann, M., Doran, M., & Wetterich, C. 2006, A & A, 454, 27

Bernet, M. L., Miniati, F., Lilly, S. J., Kronberg, P. P., & Dessauges-Zavadsky, M. 2008, Nat., 454, 302

Bowman, J. D., Morales, M. F., & Hewitt, J. N. 2006, ApJ, 638, 20

Brandenberger, R. H., Danos, R. J., Hernández, O. F., & Holder, G. P. 2010, JCAP, 12, 28

de Souza, R. S. et al. 2013, MNRAS, 432, 3218

Dewdney, P. 2013, SKA Project Documents, 1

Doran, M. & Robbers, G. 2006, JCAP, 6, 26

Durrer, R. & Neronov, A. 2013, A & A Rev., 21, 62

Evoli, C., Mesinger, A., & Ferrara, A. 2014, ArXiv e-prints

Fialkov, A., Barkana, R., Pinhas, A., & Visbal, E. 2014, MNRAS, 437, L36

Furlanetto, S. R. 2006, MNRAS, 371, 867

Giannantonio, T. et al. 2014, PRD, 89, 023511

Gordon, C. & Pritchard, J. R. 2009, PRD, 80, 063535

Hu, W. 2001, ApJ, 557, L79

Jeong, D., Schmidt, F., & Hirata, C. M. 2012, PRD, 85, 023504

Kang, X., Macciò, A. V., & Dutton, A. A. 2013, ApJ, 767, 22

Khatri, R. & Wandelt, B. D. 2007, Physical Review Letters, 98, 111301

Kunze, K. E. & Komatsu, E. 2014, JCAP, 1, 9

Lidz, A., Zahn, O., McQuinn, M., Zaldarriaga, M., & Hernquist, L. 2008, ApJ, 680, 962

Maio, U., Koopmans, L. V. E., & Ciardi, B. 2011, MNRAS, 412, L40

Mao, Y., Tegmark, M., McQuinn, M., Zaldarriaga, M., & Zahn, O. 2008, PRD, 78, 023529

McQuinn, M. & O'Leary, R. M. 2012, ApJ, 760, 3

McQuinn, M., Zahn, O., Zaldarriaga, M., Hernquist, L., & Furlanetto, S. R. 2006, ApJ, 653, 815

Mesinger, A., Ewall-Wice, A., & Hewitt, J. 2014, MNRAS, 439, 3262

Mesinger, A., Ferrara, A., & Spiegel, D. S. 2013, MNRAS, 431, 621

Metcalf, R. B. & White, S. D. M. 2009, MNRAS, 394, 704

Mineo, S., Gilfanov, M., & Sunyaev, R. 2012, MNRAS, 419, 2095

Neronov, A. & Vovk, I. 2010, Science, 328, 73

Pacucci, F., Mesinger, A., Mineo, S., & Ferrara, A. 2014, MNRAS, 443, 678

Planck Collaboration. 2013, ArXiv e-prints

Pober, J. C. et al. 2014, ApJ, 782, 66

Pourtsidou, A. & Metcalf, R. B. 2014, MNRAS, 439, L36

Pritchard, J. R. & Furlanetto, S. R. 2007, MNRAS, 376, 1680

Schleicher, D. R. G., Banerjee, R., & Klessen, R. S. 2009, ApJ, 692, 236

Sethi, S. K. & Subramanian, K. 2005, Mon. Not. Roy. Astron. Soc., 356, 778

—. 2009, Journal of Cosmology and Astro-Particle Physics, 11, 21

Shiraishi, M., Tashiro, H., & Ichiki, K. 2014, ArXiv e-prints

Sitwell, M., Mesinger, A., Ma, Y.-Z., & Sigurdson, K. 2014, MNRAS, 438, 2664

Stacy, A., Bromm, V., & Loeb, A. 2011, ApJ, 730, L1

Takahashi, K., Mori, M., Ichiki, K., Inoue, S., & Takami, H. 2013, ApJ, 771, L42

Tashiro, H. & Sugiyama, N. 2006, Mon. Not. Roy. Astron. Soc., 372, 1060

Tseliakhovich, D. & Hirata, C. 2010, PRD, 82, 083520

Valdés, M., Evoli, C., Mesinger, A., Ferrara, A., & Yoshida, N. 2013, MNRAS, 429, 1705

Viel, M., Becker, G. D., Bolton, J. S., & Haehnelt, M. G. 2013, PRD, 88, 043502

Visbal, E., Barkana, R., Fialkov, A., Tseliakhovich, D., & Hirata, C. M. 2012, Nat., 487, 70

Zahn, O. & Zaldarriaga, M. 2006, ApJ, 653, 922